ACS APPLIED MATERIALS & INTERFACES

Research Article

www.acsami.org

Multiresponsive Polymer Conetworks Capable of Responding to Changes in pH, Temperature, and Magnetic Field: Synthesis, Characterization, and Evaluation of Their Ability for Controlled Uptake and Release of Solutes

Petri Papaphilippou,[†,‡] Maria Christodoulou,[†] Oana-Maria Marinica,[§] Alina Taculescu,[⊥,∥] Ladislau Vekas,[⊥] Konstantinos Chrissafis,[#] and Theodora Krasia-Christoforou*[,†]

[†]Department of Mechanical and Manufacturing Engineering, University of Cyprus, P.O. Box 20537 1678 Nicosia, Cyprus

[§]Research Center for Engineering of Systems with Complex Fluids, University "Politehnica" Timisoara, Bd. Mihai Viteazul No. 1, 300222 Timisoara, Romania

[⊥]Center for Fundamental and Advanced Technical Research, Romanian Academy, Timisoara Branch, Bd. Mihai Viteazul, No. 24, 300223 Timisoara, Romania

[∥]Faculty of Industrial Chemistry and Environmental Engineering, University "Politehnica" Timisoara, Timisoara, Romania

[#]Department of Physics, Aristotle University of Thessaloniki, Thessaloniki, Greece

ABSTRACT: This study deals with the preparation of novel multiresponsive (magnetoresponsive, thermoresponsive and pH-responsive) nanocomposite conetworks consisting of oleic acid-coated magnetite nanoparticles (OA·Fe_3O_4), hydrophilic/thermoresponsive hexa(ethylene glycol) methyl ether methacrylate (HEGMA), hydrophobic/metal binding 2-(acetoacetoxy)ethyl methacrylate (AEMA), and pH-responsive/thermoresponsive N-diethylaminoethyl methacrylate (DEAEMA) and 2-(dimethylamino)ethyl methacrylate (DMAEMA) moieties. Conventional free radical copolymerization was employed for the synthesis of random conetworks in the absence and presence of preformed OA·Fe_3O_4. Further, in characterization of these materials in regards to their swelling behavior in organic and aqueous solvents, thermal/thermoresponsive properties, and composition, assessment of their magnetic characteristics disclosed tunable superparamagnetic behavior. These systems were also evaluated toward their ability to adsorb and release a solute (benzoic acid) in a controlled manner upon varying the pH.

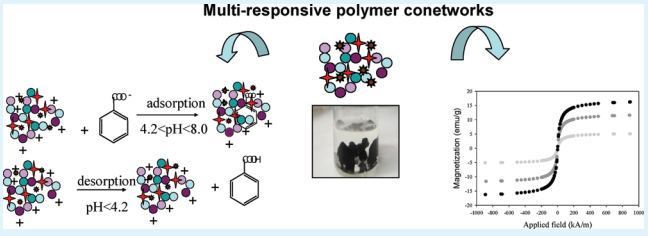

KEYWORDS: *multiresponsive composite conetworks, magnetoresponsive networks, oleic acid coated magnetite nanoparticles, superparamagnetism, pH-triggered drug delivery*

INTRODUCTION

Stimuli-responsive materials termed as "smart" materials have gained great interest because of their ability to respond to externally applied stimuli such as temperature and pH changes, light, magnetic, or electric field.[1−5] Because of this inherent property, they find significant technological and biomedical applications.[6−8]

Polymer networks are three-dimensional structures composed of polymer chains that are interconnected via chemical cross-links or physical interactions, namely covalent and physical networks, respectively. Polymer networks having the ability to respond to external changes thus altering their physical or chemical properties belong to this broad category of "smart" materials. Stimuli-responsive amphiphilic polymer networks consisting of both hydrophilic as well as hydrophobic units,[9] have the ability to absorb or retain large amount of liquids such as organic and aqueous solvents and adsorb hydrophilic as well and hydrophobic solutes. The hydrophilic units that are usually used are ionic groups or groups capable of forming hydrogen bonds. The hydrophobic regions are responsible for the swelling of the networks in organic solvents and for the adsorption of organic, hydrophobic substances. During the last decades, stimuli-responsive polymer networks have steadily attracted considerable attention in controlled drug delivery, cell sorting, catalysis, as sensors and actuators, and in bioseparation processes.[10−16]

One category of stimuli-responsive networks are the so-called pH-responsive. Within their structures, ionizable functional groups capable of responding to changes in the pH of the surrounding media are present.[17−21] These materials will swell or collapse depending on the pH of the environment. This makes pH-sensitive polymer networks particularly useful, for example, in drug delivery applications as well as in environ-

Received: January 25, 2012
Accepted: March 27, 2012
Published: March 27, 2012

mental processes, e.g., for the removal of heavy metals from aqueous waste.[22−25]

Another category of stimuli-responsive networks are those that respond to temperature changes, i.e., the thermoresponsive. Similarly to the pH-responsive systems, these materials have gained much attention in the biomedical field.[1,24,26] Polymeric materials consisting of thermo-responsive segments may undergo abrupt conformational changes upon heating above a certain critical temperature in water. For example, above a critical solution temperature defined as the lower critical solution temperature (LCST), a temperature-responsive polymer turns from hydrophilic into hydrophobic and consequently collapses in aqueous solutions.

Magnetic networks, which are frequently defined as "ferrogels" are a new class of materials comprised of swollen polymer networks in which magnetic (nano)particles are embedded. Their properties are influenced by the presence of an external magnetic field. Among the magnetic inorganic particles incorporated within polymer-based composites, superparamagnetic iron oxide nanoparticles (SPIONs) such as magnetite (Fe_3O_4) or maghemite (γ-Fe_2O_3) are by far the most commonly used.[27−34] SPIONs present many advantages especially in the biomedical field such as high contrast enhancement in magnetic resonance imaging (MRI).[35−41] Moreover, SPIONs are highly promising in hyperthermia and magnetothermally triggered drug delivery applications because by applying an alternating magnetic field, energy is released in the form of heat based on the Néel and Brownian relaxation mechanisms.[42]

Very recently, we have reported on the synthesis and characterization of nanocomposite amphiphilic random conetworks exhibiting temperature- and magneto-responsive behavior comprised of hexa(ethylene glycol) methyl ether methacrylate (HEGMA, hydrophilic, thermoresponsive), 2-(acetoacetoxy)ethyl methacrylate (AEMA, hydrophobic, metal-chelating), and oleic acid-coated magnetite nanoparticles (OA·Fe_3O_4).[43]

Giving further credence to this approach, herein we describe the synthesis and characterization of triple-responsive nanocomposite conetworks (magnetoresponsive, thermoresponsive, and pH-responsive). The possibility of using temperature, magnetic field, and pH stimuli to control the response of a single system is considered to be highly advantageous for their future exploitation in the biomedical field.

These materials consist of: (a) hydrophilic, biocompatible, and thermoresponsive hexa(ethylene glycol) methyl ether methacrylate (HEGMA) units, (b) hydrophobic 2-(acetoacetoxy)ethyl methacrylate (AEMA) units bearing β-ketoester metal-chelating functionalities, (c) pH-responsive moieties, *N*-diethylaminoethyl methacrylate (DEAEMA), and 2-(dimethylamino)ethyl methacrylate (DMAEMA) and (d) oleic acid-coated iron oxide nanoparticles (OA·Fe_3O_4), combined all together in a random conetwork architecture.

HEGMA was chosen to be the hydrophilic component within the conetwork due to its biocompatibility and its thermoresponsive properties.[44] AEMA hydrophobic moieties containing β-ketoester side-chain functionalities, were introduced because of their ability to bind effectively onto the inorganic iron oxide surfaces providing an improved stabilization.[45−47] Moreover, the incorporation of the pH-responsive DEAEMA and pH- and thermoresponsive DMAEMA units capable of becoming positively charged below their pK_a values (8 and 7.3 for polyDMAEMA and polyDEAEMA respectively)[48,49] provided the possibility to evaluate these systems in controlled, pH-triggered drug delivery processes. Finally, the preference of incorporating preformed, oleic acid (OA)-coated magnetite nanoparticles with mean diameters of around 4−5 nm[43] within the conetworks targeted toward a superparamagnetic response.

Conventional free radical polymerization was employed for the fabrication of the OA·Fe_3O_4-containing nanocomposite conetworks in a single synthetic step. Ethylene glycol dimethacrylate (EGDMA) was used as the cross-linker, whereas 2,2′-azobis(2-methylpropionitrile) (AIBN) served as the radical source. Besides their characterization to determine their compositional, swelling, thermal, and magnetic properties, the conetworks were further evaluated toward their ability to adsorb and release benzoic acid in a controlled manner upon varying the pH. The latter, combined with their superparamagnetic behavior and thermoresponsive properties render them promising materials in the biomedical field as multiresponsive, externally actuated drug delivery systems.

EXPERIMENTAL SECTION

Chemicals and Reagents. Tetrahydrofuran (THF, Scharlau, HPLC grade), NH_4OH (Scharlau, 25% (v/v) H_2O), 2-(dimethylamino)ethyl methacrylate (DMAEMA, Sigma-Aldrich, 99%), *N*-diethylaminoethyl methacrylate (DEAEMA, Sigma-Aldrich, 99%), and the polymerization cross-linker ethylene glycol dimethacrylate (EGDMA, Sigma-Aldrich, 99%) were used as received. The radical initiator 2,2′-azobis(2-methylpropionitrile) (AIBN, Sigma-Aldrich, 95%) was recrystallized twice from ethanol. 2-(Acetoacetoxy) ethyl methacrylate (AEMA; Sigma-Aldrich, 95%) was passed through a basic alumina column prior to the polymerizations and used without further purification. Similarly, hexa(ethylene glycol) methyl ether methacrylate (HEGMA, molecular weight (MW) 300, n = 6; Sigma-Aldrich) after being diluted in tetrahydrofuran (THF) was allowed to pass through a basic alumina column. THF was evaporated off and HEGMA was used without further purification. Oleic acid (Merck, 99%), iron sulfate (II) heptahydrate (Sigma-Aldrich, 97%) and iron chloride (III) tetrahydrate (Sigma-Aldrich, 99%) were used as provided by the manufacturer.

Oleic Acid-Coated Magnetite Nanoparticles. The oleic acid-coated magnetite nanoparticles (OA·Fe_3O_4) were prepared at the Center for Fundamental and Advanced Technical Research, Romanian Academy, Timisoara Branch, Romania, by following an experimental procedure developed by Bica et al.[50−52] Briefly, magnetite nanoparticles, Fe_3O_4, were obtained by the coprecipitation in aqueous solution of Fe^{2+} and Fe^{3+} ions (salts $FeSO_4·7H_2O$ and $FeCl_3·4H_2O$) in the presence of NH_4OH at 80−82 °C. The temperature of 80 °C set for the coprecipitation reaction is essential to obtain magnetite and not other iron oxides;[50] the same temperature range is also favorable for the chemisorption of oleic acid on the surface of magnetite nanoparticles.[41,53] In addition, the significant excess amount of NH_4OH ensures the formation of magnetite over other iron oxides. However, very slow oxidation of magnetite to maghemite cannot be excluded as a long-term process. Subsequently, oleic acid was added in a significant excess amount (∼ 30 vol%) to the system right after the coprecipitation had started, which resulted in the chemisorption of the acid on the magnetite surface. This was followed by a washing process with distilled water with magnetic decantation and filtration to remove aggregated (nondispersed) particles. Then, flocculation (acetone) was used to extract magnetite particles coated with a single surfactant layer from the solution of residual salts and free surfactant. The dried powder was redispersed in light hydrocarbon. This flocculation/redispersion procedure was performed several times to ensure that the presence of free surfactant in the final solution was negligible.

HEGMA-co-AEMA-co-DEAEMA-co-DMAEMA/EGDMA Random Conetworks. Free radical cross-linking copolymerization was employed for the synthesis of the HEGMA-co-AEMA-co-DEAEMA-

Table 1. Quantities of the Chemical Reagents Used in the Fabrication of the (Composite) Conetworks (Solvent, Monomers, Crosslinker, Initiator, and OA·Fe_3O_4) and Corresponding Sol Fraction Percentages

	HEGMA		AEMA		DEAEMA		DMAEMA		EGDMA		AIBN				
sample ID	mL	mmol	mL	mmol	mL	mmol	mL	mmol	mL	mmol	mg	mmol	THF (mL)	OA· Fe_3O_4 (g)	sol fraction (%)
X1	1.90	7.00	1.34	7.00	1.40	7.00	1.18	7.00	3.20	17.0	32.8	0.20	24		9.45
X2	0.95	3.50	0.67	3.50	0.70	3.50	0.59	3.50	1.60	8.50	16.4	0.10	22	1.17	20.21
X3	0.95	3.50	0.67	3.50	0.70	3.50	0.59	3.50	1.60	8.50	16.4	0.10	33	2.01	25.38
X4	0.48	1.75	0.34	1.75	0.35	1.75	0.29	1.75	0.80	4.25	8.2	0.05	27	1.56	24.20

co-DMAEMA/EGDMA random conetworks. Polymerizations were carried out in a 50 mL round-bottom flask, fitted with a rubber septum. The monomers HEGMA (2.1 g, 7.0 mmol), AEMA (1.5 g, 7.0 mmol), DMAEMA (1.1 g, 7.0 mmol), DEAEMA (1.29 g, 7.0 mmol), and the cross-linker EGDMA (3.37 g, 17 mmol) were transferred to the reaction flask with the aid of a syringe. THF (24 mL) was subsequently added followed by the addition of the initiator AIBN (0.0328 g, 0.2 mmol) dissolved in the solvent (4 mL). The reaction mixture was placed in an oil bath at 63 °C. Gelation was reached within 21 h. The prepared conetwork was taken out of the polymerization flask and was left to equilibrate in THF (100 mL) for 1 week to remove the sol fraction (extractables). Subsequently, the solvent was recovered by filtration and evaporated off under reduced pressure. The recovered extractables were dried under vacuum at room temperature for 24 h. The sol fraction was calculated as the ratio of the dried mass of the extractables divided by the theoretical mass of all components in the network (i.e., the monomers plus the cross-linker).

OA·Fe_3O_4-Containing Nanocomposite Conetworks. A typical procedure followed for the preparation of OA·Fe_3O_4-containing nanocomposite conetworks is described as follows: At first, the monomers HEGMA (1.05 g, 3.5 mmol), AEMA (0.75 g, 3.5 mmol), DMAEMA (0.55 g, 3.5 mmol), DEAEMA (0.64 g, 3.5 mmol) and OA·Fe_3O_4 (1.174 g for X2) were placed into a 100 mL round-bottom flask. Subsequently, sonication was applied for 1 h to assist homogeneous mixing. THF (22 mL), EGDMA (1.68 g, 8.5 mmol) and AIBN (0.0164 g, 0.1 mmol) dissolved in THF (4 mL) were then transferred to the reaction flask with the aid of a syringe. The reaction mixture was placed in an oil bath at 63 °C. Gelation was reached within 19 h. It is noteworthy to mention at this point that the gelation process was slower upon increasing the magnetic content. The prepared composite conetwork was taken out of the polymerization flask and was left to equilibrate in THF (100 mL) for 1 week to remove the sol fraction (extractables). Subsequently, the solvent was recovered by filtration and evaporated off under reduced pressure. The recovered extractables were dried under vacuum at room temperature for 24 h and their mass was determined gravimetrically. Table 1 summarizes the quantities of the chemical reagents used to prepare the conetworks (solvent, monomers, cross-linker, initiator and OA·Fe_3O_4) together with the corresponding sol fraction percentage. The latter was calculated as the ratio of the dried mass of the extractables (organic and inorganic substances—possibly unreacted monomers, cross-linker, and OA·Fe_3O_4 not incorporated into the conetworks) divided by the theoretical mass of all components in the conetwork (i.e., the monomers, the cross-linker, and the OA·Fe_3O_4).

Determination of the Degree of Swelling. The washed conetworks were cut into small pieces and their THF-swollen mass was determined gravimetrically before placing all samples in a vacuum oven for drying for 24 h at room temperature. The dry conetwork mass was then determined, followed by the transfer of the conetworks in neutral water. All conetworks remained stable in the aqueous phase. The mass of the swollen conetworks was determined gravimetrically 5, 10, and 14 days after placing a dried sample in neutral water to ensure that the conetwork has reached the equilibrium state. Since no swelling differences were observed during the last two measurements, all samples were left to equilibrate in aqueous solutions for 2 weeks and the water-swollen conetwork masses were measured. Leakage of OA.Fe_3O_4 from the water-swollen hydrogels was not observed for long time periods (longer than 3 months). The DSs were calculated as the ratio of the swollen conetwork mass divided by the dry conetwork mass.

Deswelling Measurements. Deswelling studies were performed on sample X3 (30 wt % OA·Fe_3O_4) in water. After letting the sample to equilibrate for 2 weeks in distilled water at 25 °C, the swollen gel was transferred into water at 60 °C and its weight was recorded at different time intervals. The water content at each time interval was determined as W_t/W_0, where W_t corresponds to the weight of the swollen conetwork at a designated time t during deswelling and W_0 to the weight of the conetwork measured initially at 25 °C.

Adsorption/Desorption Kinetic Studies. The adsorption − desorption kinetics of the benzoic acid was investigated by means of UV−vis spectroscopy, by recording the characteristic absorption signals of the solute appearing at 230 and 270 nm at different time intervals. In the adsorption experiments, the polymer conetworks X1 (no OA·Fe_3O_4) and X2 (20 wt %) preswelled in an aqueous solution of a pH ∼ 4.3 and ∼4.7, respectively (5 mL), were placed in a vial containing an aqueous solution of benzoic acid (∼2 mg in 10 mL of deionized water). At specific times the solution was removed from the vial and it was placed in the UV−vis spectrophotometer for recording the spectrum. After each measurement, the solution was placed back into the vial. The whole procedure was repeated several times. Similarly, in the desorption experiments, samples X1/benzoic acid and X2/benzoic acid were placed separately in two vials containing 5 mL of acidified water (pH ∼2.8). In both cases, the solutions were removed from the vials, placed in the UV−vis spectrophotometer for recording the spectrum at each time interval and then placed back again into the vials.

Instrumentation. X-ray diffraction spectroscopy experiments were carried out on an XRD instrument (Rigaku, 30 kV, 25 mA with λ = 1.5405 Å (Cu), goniometer type: vertical) in the range of 5 to 90° and at a scanning rate of 0.5°/min. Thermogravimetric analysis was carried out with a SETARAM SETSYS TG-DTA 16/18. Samples (6.0 ± 0.2 mg) were placed in alumina crucibles. An empty alumina crucible was used as a reference. The samples were heated from ambient temperature to 500 °C in a 50 mL/min flow of Ar at a heating rate of 10 °C/min. The magnetic properties of the nanocomposite conetworks were measured with a vibrating sample magnetometer model 880 from ADE Technologies USA. The adsorption/desorption kinetic studies were performed on a Jasco V − 630 UV−vis Spectophotometer operating at room temperature.

RESULTS AND DISCUSSION

Synthesis. The chemical structures and names of monomers and cross-linker used in the fabrication of the HEGMA-co-AEMA-co-DEAEMA-co-DMAEMA/EGDMA random conetworks are illustrated in Figure 1.

For the synthesis of the OA·Fe_3O_4-containing nanocomposite conetworks, the same synthetic approach as that recently reported by our group was followed,[43] involving the free radical random copolymerization of all monomers and the cross-linker carried out in the presence of preformed OA.Fe_3O_4. As already mentioned in the Experimental Section, the latter were prepared by following the chemical coprecipitation of Fe(II) and Fe(III) salts in the presence of NH_4OH at elevated temperatures, leading to the formation of

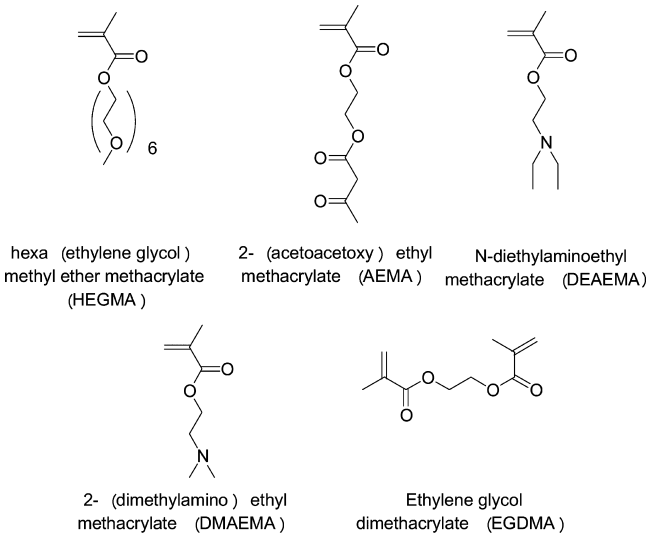

Figure 1. Chemical structures and names of the monomers and cross-linker used in conetwork synthesis via free radical polymerization.

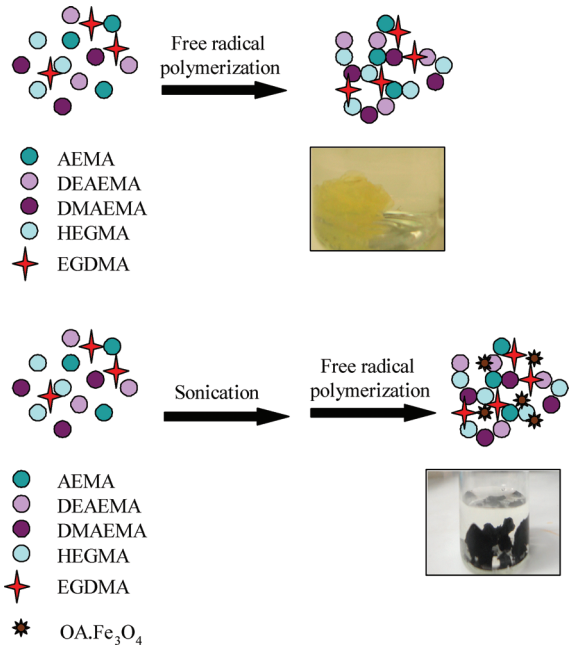

Figure 2. Schematic illustration of the synthetic methodology followed for the fabrication of: (a) HEGMA-co-AEMA-co-DEAEMA-co-DMAEMA/EGDMA random conetworks and (b) nanocomposite polymer/OA·Fe_3O_4 conetworks.

magnetite nanoparticles characterized by average diameters of ~5 nm.[43]

Four conetworks were prepared in total, one in the absence and three in the presence of OA·Fe_3O_4: X1, no OA·Fe_3O_4; X2, 20 wt % OA×Fe_3O_4; X3, 30 wt % OA·Fe_3O_4, and X4, 40 wt % OA·Fe_3O_4. Because all monomers incorporated within the conetworks are methacrylates, similar reactivity ratios and therefore structural "randomness" is expected for the conetworks. It should be mentioned at this point that the gelation process was slower upon increasing the magnetic content; gelation was reached within 19, 43, and 168 h for X2, X3, and X4, respectively.

Figure 2 illustrates the methodology followed for the preparation of the aforementioned systems.

Table 2. Degrees of Swelling (DS) of the Conetworks in the Presence and Absence of OA·Fe_3O_4, Determined in Aqueous Media at Different pHs and in THF, Together with the 95% Confidence Intervals

sample ID	pH	$DS_{aqueous}$	DS_{THF}
X1 (no OA·Fe_3O_4)	1.6	2.8 ± 0.01	4.10
	3.8	2.4 ± 0.01	
	8.1	2.0 ± 0.03	
	9.7	1.9 ± 0.01	
X2 (20% OA·Fe_3O_4)	2.2	2.91 ± 0.01	6.95
	4.3	4.37 ± 0.04	
	5.6	4.89 ± 0.01	
X3 (30% OA·Fe_3O_4)	1.9	2.90 ± 0.01	6.75
	5.3	4.75 ± 0.02	
	9.7	5.42 ± 0.01	
X4 (40% OA·Fe_3O_4)	1.6	2.87 ± 0.01	6.15
	4.7	4.48 ± 0.01	
	7.4	5.38 ± 0.01	
	10.2	5.65 ± 0.01	

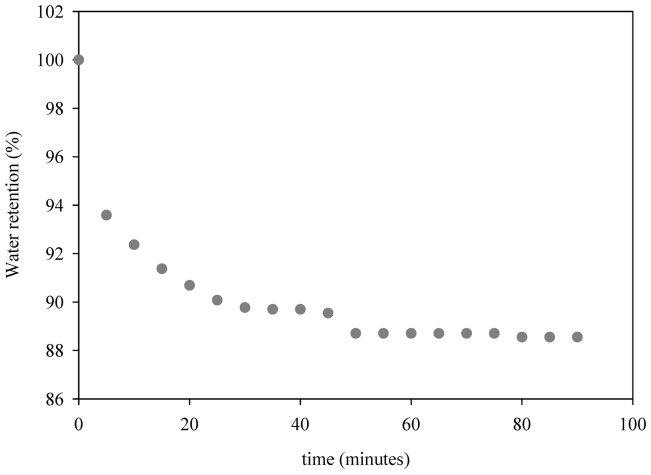

Figure 3. Deswelling kinetic plot of sample X3 (HEGMA-co-AEMA-co-DEAEMA-co-DMAEMA/EGDMA with 30 wt % Fe_3O_4) recorded in water at ~60 °C.

The sol fraction (extractables) of the conetworks was relatively high and varied from ~10% for the conetwork

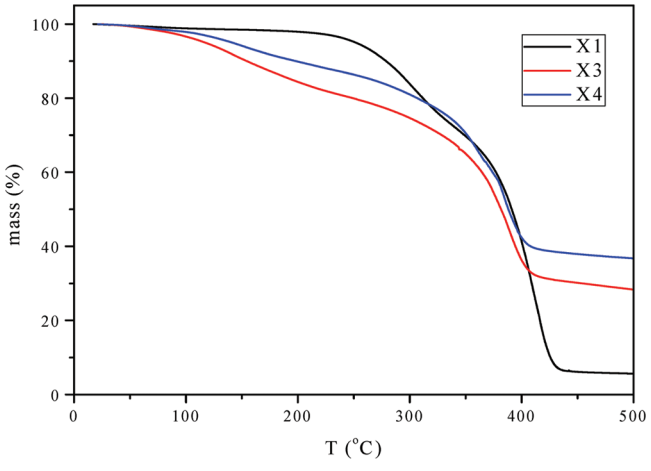

Figure 4. TGA thermograms of X1 (no OA·Fe_3O_4), X3 (OA·Fe_3O_4, 30 wt %), and X4 (OA·Fe_3O_4, 40 wt %).

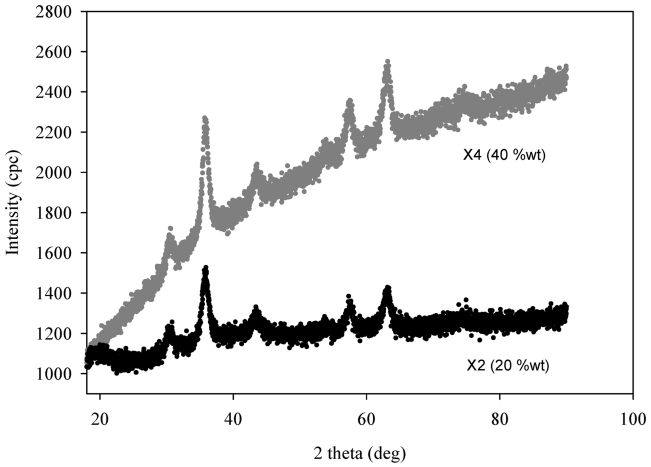

Figure 5. X-ray diffraction patterns of samples X2 (OA.Fe_3O_4, 20 wt %) and X4 (OA·Fe_3O_4, 40 wt %).

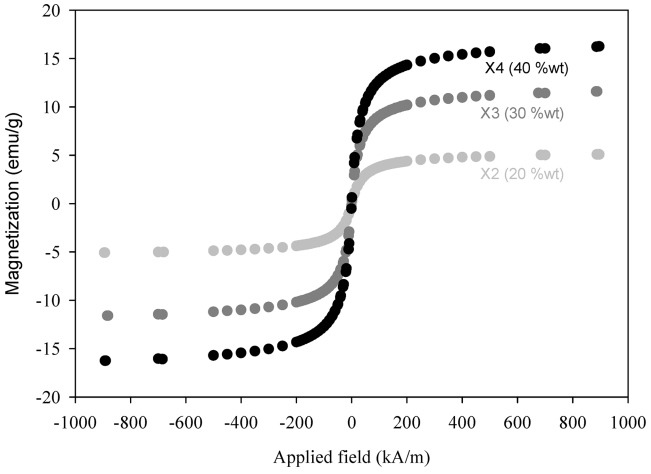

Figure 6. Magnetization curves corresponding to samples X2- light gray (OA·Fe_3O_4, 20 wt %), X3-dark gray (OA·Fe_3O_4, 30 wt %), and X4-black (OA·Fe_3O_4, 40 wt %).

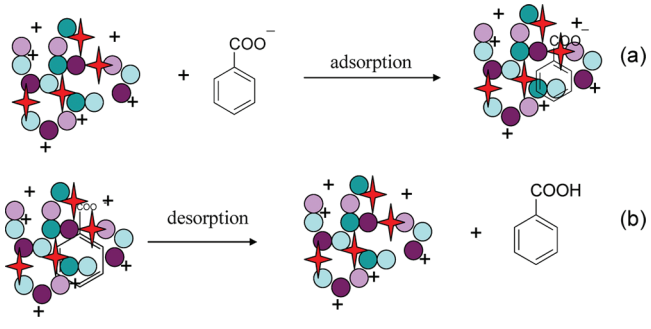

Figure 7. (a) Adsorption and (b) desorption of benzoic acid onto and from the conetworks, respectively.

prepared in the absence of the OA·Fe_3O_4 to ~20% wt for the conetworks synthesized in the presence of OA·Fe_3O_4. This is consistent with our previous findings,[43] where the lowest percentage of extractables was observed in the case where the gelation of HEGMA and AEMA in the presence of the EGDMA cross-linker was carried out in the absence of the OA·Fe_3O_4.

Swelling Behavior. The degrees of swelling (DS) of the conetworks were determined in THF and in aqueous media of various pHs. Table 2 summarizes the DS together with the 95% confidence intervals.

The DS determined in aqueous media was in all cases lower compared to those determined in THF. This is attributed to the fact that THF is a good solvent for all units that are present within the conetwork, whereas water is only selective for the HEGMA (at all pHs), DMAEMA (at all pH levels), and DEAEMA (at pH $\lesssim$7) units.

In the case of X1 (no OA·Fe_3O_4), the DS was found to increase as the pH decreased. This phenomenon has been previously observed for DMAEMA-containing polymer conetworks and has been attributed to the ionization of the DMAEMA units at low pH, causing electrostatic repulsion effects between the network chains.[54] Moreover, swelling at lower pHs is further promoted upon the establishment of an osmotic pressure within the network because of the accumulation of the chloride counterions.

Magnetite is an amphoteric solid that can be subjected to changes of its surface charge (protonation and deprotonation) upon varying the pH, according to the following chemical equations[55]

$$Fe - OH + H^+ \Leftrightarrow Fe - OH_2^+ [\text{protonation}]$$

$$Fe - OH \Leftrightarrow Fe - O^- + H^+ [\text{deprotonation}]$$

At low pH values, the surface of the magnetite becomes protonated and hydrophobic, whereas at high pH values, negative charges are generated onto its surface, rendering it hydrophilic. At a pH of ~8.0 (the so-called point of zero charge, (PZC)) the surface of the magnetite is neutral. As seen in Table 2, the DS of the magnetite-containing conetworks increases with pH with the highest DS values being observed at pH >8. On the basis of the aforementioned, an explanation for this behavior might be the promotion of the generation of a more hydrophilic surface onto the embedded magnetite nanoparticles at higher pHs, promoting further swelling of the conetworks in aqueous solutions.

Thermal Properties. *Thermoresponsive Character.* Many examples appearing in the literature report on the thermoresponsive behavior of polymeric materials comprised of oligo(ethylene glycol) side-chain segments.[44,45] These materials display the so-called lower critical solution temperature (LCST) in aqueous media i.e. they have the ability to turn from hydrophilic into hydrophobic upon temperature increase above the LCST. In a recent publication, we have demonstrated the thermoresponsive character of HEGMA-co-AEMA/EGDMA conetworks with embedded OA.Fe_3O_4 nanoparticles in aqueous solution.[43] Similarly, in the present work after transferring the conetworks from their swollen state in neutral water at ambient temperature into preheated water at 60 °C, deswelling was observed. The kinetics of the deswelling process could be followed upon measuring the mass decrease of the conetworks at various time intervals. Exemplarily, the deswelling kinetic plot for gel X3 (30% OA.Fe_3O_4) is presented in Figure 3.

Thermal Stability. For determining the decomposition temperatures of the polymer conetworks in the absence and presence of the magnetic nanoparticles, TGA measurements were carried out. Exemplarily, the TGA traces of X1 (no OA·Fe_3O_4), X3 (OA·Fe_3O_4, 30 wt %) and X4 (OA·Fe_3O_4, 40 wt %) are provided in Figure 4. As seen in the figure, the pristine polymer conetwork begins to decompose at ~200 °C, whereas at ~500 °C the decomposition is completed, leaving a

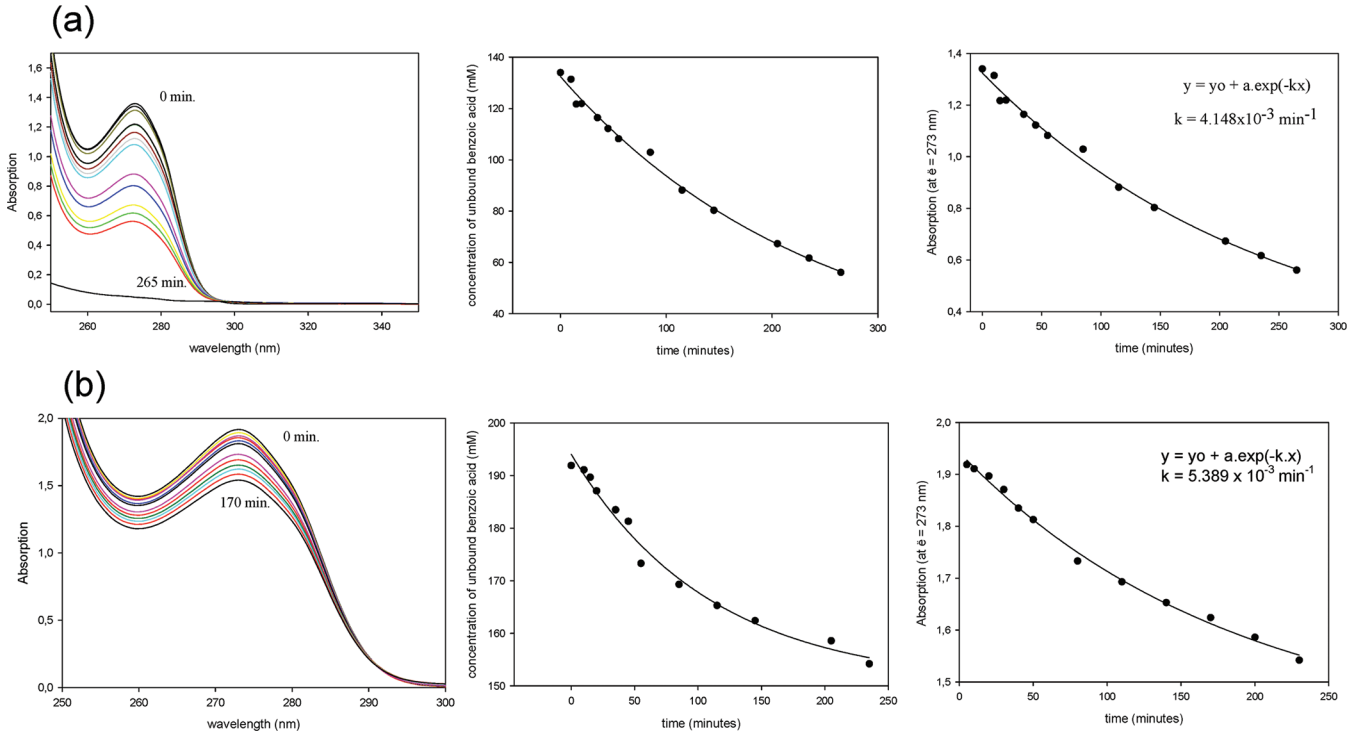

Figure 8. Adsorption kinetics of benzoic acid into (a) X1 (no OA·Fe_3O_4) and (b) X2 (OA·Fe_3O_4, 20 wt %) conetworks at pH ∼ 4.3 and ∼4.7, respectively: UV−vis spectra, concentration versus time, and absorption versus time plots.

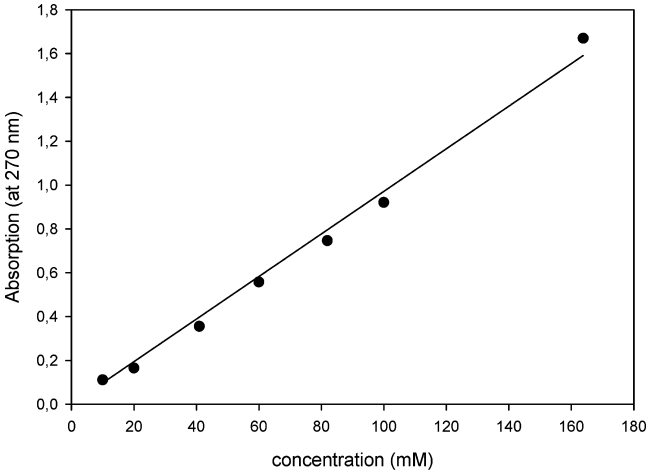

Figure 9. Absorption (at λ = 270 nm) versus concentration calibration curve for benzoic acid in aqueous media.

small residue. A similar observation i.e. noncomplete calcination of the organic material at this temperature range was carried out by J.M. Cervantes-Uc et al. who investigated the thermal degradation behavior of polymethacrylates containing amine side chain groups.[56] In the case of X3 and X4 at the same temperature, the remaining residue corresponds almost to the magnetic content.

Nanocrystalline Phase Characterization. X-ray diffraction (XRD) spectroscopy was used to investigate the nanocrystalline phase adopted by the magnetic nanoparticles embedded within the polymer conetworks. The powder XRD diffraction patterns of the composite conetworks X2 (OA·Fe_3O_4, 20 wt %) and X4 (OA·Fe_3O_4, 40 wt %) are presented in Figure 5. Six broad peaks appearing at $\theta \sim 30$, 36, 43, 54, 58, and 63° are displayed in both cases in the XRD patterns, indicating the presence of magnetite (Fe_3O_4) within the composite conetworks.[57−59]

Magnetic Response. Vibrating sample magnetometry (VSM) measurements performed at 300 K provided information on the magnetic behavior of the composite conetworks. Figure 6 shows the magnetization (M) versus applied magnetic field strength (H) plots for all composite conetworks (X2, X3, and X4). The magnetic measurement studies demonstrated the superparamagnetic behavior of these materials since the magnetization plots were characterized by a symmetrical and sigmoidal shape and hysteresis was absent. Moreover, from the magnetization plots it becomes obvious that upon increasing the magnetic content within the conetworks, the saturation magnetization (M_s) increases as expected, whereas the superparamagnetic properties are retained.

pH-Triggered Uptake and Release. The presence of DMAEMA and DEAEMA pH-responsive functionalities within the conetworks provided the possibility to explore their applicability as pH-triggered systems for the controlled adsorption and release of solutes in aqueous media of appropriate pH. The adsorption mechanism is based on the development of electrostatic attractive forces taking place between the conetworks and the solute, whereas the release of the latter can be achieved *via* the destruction of these interactions.

Benzoic acid was selected as a model compound to be used in the uptake and release studies. This molecule has a pK_a value of ∼4.2; that means that below this value it is found in its neutral (nonionic) form, whereas above it, it gets deprotonated and becomes negatively charged. On the other hand, the DMAEMA and DEAEMA units become positively charged below pH ∼7 (pK_a of pDMAEMA ∼8[48] and pK_a of pDEAEMA ∼7.3.[49] On the basis of the above, it is expected that in the pH

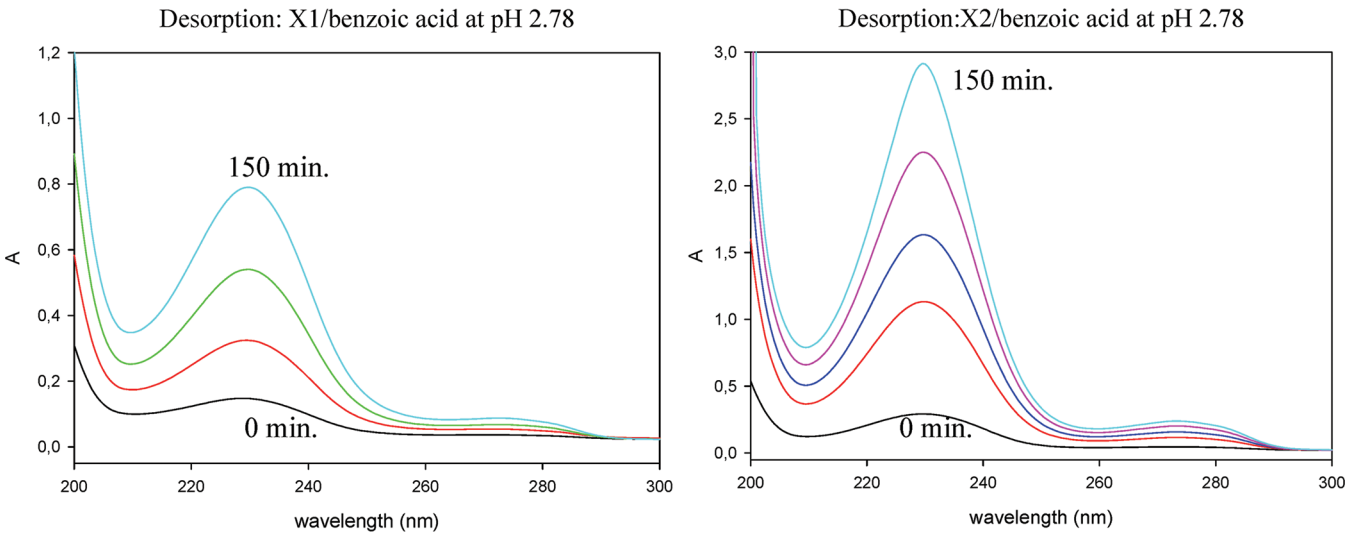

Figure 10. Desorption kinetics of benzoic acid from the X1/benzoic acid and X2/benzoic acid systems at pH ∼2.8.

range 4.2 < pH < 8, the benzoic acid molecules will be adsorbed by the conetwork since at this range, the former will possess a negative charge whereas the latter will be positively charged, as schematically presented in Figure 7a.

Adsorption kinetic measurements were carried out in aqueous solutions at a pH slightly above the pK_a of the benzoic acid (4.3−4.7) by UV−vis spectrophotometry. As already described in the Experimental Section, the characteristic absorption signals of the benzoic acid appearing at 230 and 270 nm were recorded at different time intervals after immersing the X1 (no OA.Fe_3O_4) and X2 (20% wt. OA.Fe_3O_4) conetworks preswelled in an aqueous solution of a pH ∼4.3 and ∼4.7, respectively in vials containing an aqueous solution of benzoic acid. Figure 8 shows the UV−vis spectra and corresponding absorption versus time ($A = f(t)$) plots for the above-mentioned cases. In both cases, the absorption signal of the benzoic acid that is found free in solution appearing at 270 nm decreases with time, demonstrating the successful incorporation of this solute within the conetwork. By comparing the adsorption kinetics for these 2 cases, it can be seen that the adsorption process is slower in the case of the conetwork X2 in which magnetite nanoparticles are embedded. A possible explanation for this might be the hydrophobic nature of the surface of the magnetite nanoparticles at this pH range that may disfavor the incorporation of the ionized benzoic acid within the conetwork.

By measuring the absorption of benzoic acid aqueous solutions of known concentrations at the maximum absorption wavelength (∼270 nm), it was possible to construct the absorption versus concentration calibration curve for benzoic acid, as depicted in Figure 9.

Using the Beer−Lambert law: $A_{\lambda max} = \varepsilon cd$ (where $A_{\lambda max}$ is the absorption at the maximum wavelength, ε is the absorption coefficient, c is the solute concentration, and d is the path length), quantitative data, i.e., the concentration of benzoic acid found free in solution as a function of time, could be extracted (Figure 8).

Even though in the present work no experiments were carried out for correlating the adsorption kinetics with the pH or the presence of saline, it is expected that both parameters will affect the adsorption process.

The pH significantly affects the degree of ionization of the groups involved in the development of electrostatic interaction forces. Therefore it is expected that adsorption kinetics will be faster at pH values that promote the generation of positive charges onto the conetworks (DMAEMA/DEAEMA units) and of a negatively charged solute (anionized benzoic acid). Similarly, Patrickios and co-workers[60] investigated the pH-dependence of the adsorption of various proteins on DMAEMA-containing model conetworks and demonstrated that protein adsorption takes place only when the DMAEMA units and the protein have an opposite charge.

The presence of saline has an influence on the ionic strength and therefore the degree of swelling of ionic networks.[23] In addition, when an electrostatically bound polymer-solute system is placed in saline (e.g., NaCl solution) drug release may occur due to displacement effects of the ionic solute by the ionic salt. Such an observation has been reported by Sutani et al. in the case of release of an ionic drug from a polyampholyte gel.[61] Although no release of an anionically bound drug was observed in distilled water, when the polymer-drug system was placed into isotonic sodium chloride solution, drug dissociation, and release occurred.

Upon immersing the X1/benzoic acid and X2/benzoic acid samples in acidified water (pH∼ 2.8) and recording the UV−vis spectra of the supernatant solution, a systematic increase in the absorption signal appearing at ∼230 nm corresponding to the free benzoic acid molecules released from the conetwork is observed in both cases. The release process is attributed to the protonation and thus neutralization of the benzoic acid molecules encapsulated within the conetwork at such low pH values, resulting to the destruction of the electrostatic attractive forces taking place between the conetwork and the solute and the release of the latter, as schematically presented in Figure 7b.

CONCLUSIONS

Conclusively, we have described the synthesis and characterization of multiresponsive random conetworks based on functional methacrylate monomers and oleic-acid-coated Fe_3O_4 nanoparticles. A simple synthetic approach was followed for the preparation of these new systems involving the free radical cross-linking copolymerization of three functional monomers possessing pH-responsive (DEAEMA/DMAEMA),

thermoresponsive (HEGMA, DMAEMA) and metal binding (AEMA) moieties in the presence of preformed oleic acid-coated magnetite nanoparticles. The incorporation of the temperature responsive HEGMA and DMAEMA units affords materials capable of responding to temperature changes i.e. deswell in aqueous solutions at specific temperatures. The presence of embedded oleic acid-coated magnetite nanoparticles within the conetworks, leads to nanocomposite materials that demonstrate superparamagnetic behavior in the presence of an externally applied magnetic field. Moreover, the introduction of pH-responsive moieties renders these systems capable of responding to pH changes. On the basis of the latter, in the present work, it has been demonstrated that benzoic acid can be adsorbed by the conetworks and released in a controlled manner under certain pH conditions.

The ability of these materials to adsorb and desorb solutes in a controlled manner upon triggering the pH, combined with their tunable superparamagnetic behavior and thermoresponsive properties in aqueous media, may allow for their future exploitation in the biomedical field.

AUTHOR INFORMATION

Corresponding Author

*E-mail: krasia@ucy.ac.cy.

Present Address

‡Department of Civil and Environmental Engineering, University of Cyprus.

Notes

The authors declare no competing financial interest.

ACKNOWLEDGMENTS

This work was supported by the University of Cyprus and the Romanian Academy-Timisoara Branch. We thank Ms. C. Papageorgiou and Dr. T. Kyratsi (Department of Mechanical and Manufacturing Engineering, University of Cyprus) for the assistance with the XRD measurements.

REFERENCES

(1) Fang, L.; Urban, M. W. *Prog. Polym. Sci.* **2010**, 3−23.
(2) Meenach, S. A.; Anderson, K. W.; Hilt, J. Z. *J. Polym. Sci., Part A: Polym. Chem.* **2010**, *48*, 3229−3235.
(3) Kulkarni, R. V.; Biswanath, S. J. *Appl. Biomater. Biomech.* **2007**, *5*, 125−139.
(4) You, J.-O.; Almeda, D.; JC Ye, G.; Auguste, D. T. *J. Biol. Eng.* **2010**, *4*, 15.
(5) Schmaljohann, D. *Adv. Drug Delivery Rev.* **2006**, *58*, 1655−1670.
(6) Bajpai, A. K.; Bajpai, J.; Saini, R.; Gupta, R. *Polym. Rev.* **2011**, *51*, 53−97.
(7) Resendiz-Hernandez, P. J.; Rodriguez-Fernandez, O. S.; Garcia-Cerda, L. A. *J. Magn. Magn. Mater.* **2008**, *320*, E373−E376.
(8) Cohen Stuart, M. A.; Huck, W. T. S.; Genzer, J.; Müller, M.; Ober, C.; Stamm, M.; Sukhorukov, G. B.; Szleifer, I.; Tsukruk, V. V.; Urban, M.; Winnik, F.; Zauscher, S.; Luzinov, I.; Minko, S. *Nat. Mater.* **2010**, *9*, 101−113.
(9) Patrickios, C. S.; Georgiou, T. K. *Curr. Opin. Colloid Interface Sci.* **2003**, *8*, 76−85.
(10) Bajpai, A. K.; Shukla, S. K.; Bhanu, S.; Kankane, S. *Prog. Polym. Sci.* **2008**, *33*, 1088−1118.
(11) Bawa, P.; Pillay, V.; Choonara, Y. E.; Du Toit, L. C. *Biomed. Mater.* **2009**, *4*, No. 022001.
(12) Sahiner, N. *Colloid Polym. Sci.* **2006**, *285*, 283−292.
(13) Dong, L.; Jiang, H. *Soft Matter* **2007**, *3*, 1223−1230.
(14) Liu, T.-Y.; Hu, S.-H.; Liu, K.-H.; Liu, D.-M.; Chen, S.-Y. J. *Controlled Release* **2008**, *126*, 228−236.
(15) Liu, T. Y.; Hu, S.-H.; Liu, T.-Y.; Liu, D.-M..; Chen, S.-Y. *Langmuir* **2006**, *22*, 5974−5978.
(16) Liang, Y. Y.; Zhang, L. M.; Jiang, W. *Chem. Phys. Chem.* **2007**, *8*, 2367−2372.
(17) Tian, P.; Wu, Q.; Lia, K. J. *Appl. Polym. Sci.* **2008**, *108*, 2226−2232.
(18) Orakdogen, N. *Polym. Bull.* **2011**, *67*, 1347−1366.
(19) Medeiros, S. F.; Santos, A. M.; Fessi, H.; Elaissari, A. *Int. J. Pharm.* **2011**, *403*, 139−161.
(20) Karg, M.; Lu, Y.; Carbó-Argibay, E.; Pastoriza-Santos, I.; Pérez-Juste, J.; Liz-Marzán, L. M.; Hellweg, T. *Langmuir* **2009**, *25*, 3163−3167.
(21) Karl Kratz, K.; Hellweg, T.; Eimer, W. *Colloids Surf., A* **2000**, *170*, 137−149.
(22) Mano, J. F. *Adv. Eng. Mater.* **2008**, *10*, 515−527.
(23) Gupta, P.; Vermani, K.; Garg, S. *Drug Discovery Today* **2002**, *7*, 569−579.
(24) Tomic, S. LJ.; Micic, M. M.; Dobic, S. N.; Filipovic, J. M.; Suljovrujic, E. H. *Radiat. Phys. Chem.* **2010**, *79*, 643−649.
(25) Paulino, A. T.; Belfore, L. A.; Kubota, L. T.; Muniz, E. C.; Almeida, V. C.; Tambourgi, E. B. *Desalination* **2011**, *275*, 187−196.
(26) Jones, J. A.; Novo, N.; Flagler, K.; Pagnuccos, C. D.; Carew, S.; Cheong, C.; Kong, X. Z.; Burke, N. A. D.; Stover, H. D. H. *J. Polym. Sci., Part A: Polym. Chem.* **2005**, *43*, 6095−6104.
(27) Starodoubtsev, S. G.; Saenko, E. V.; Khokhlov, A. R.; Volkov, V. V.; Dembo, K. A.; Klechkovskaya, V. V.; Shtykova, E. V.; Zanaveskina, I. S. *Microelectron. Eng.* **2003**, *69*, 324−329.
(28) Paquet, C.; De Haan, H. W.; Leek, D. M.; Lin, H.-Y.; Xiang, B.; Tian, G.; Kell, A.; Simard, B. *ACS Nano* **2011**, *5*, 3104−3112.
(29) Meenach, S. A.; Hilt, J. Z.; Anderson, K. W. *Acta Biomater.* **2010**, *6*, 1039−1046.
(30) Meenach, S. A.; Anderson, A. A.; Suthar, M.; Anderson, K. W.; Hilt, J. Z. *J. Biomed. Mater. Res. Part A* **2009**, *91A*, 903−909.
(31) Sivudu, K. S.; Rhee, K. Y. *Colloids Surf., A* **2009**, *349*, 29−34.
(32) Sauzedde, F.; Elaissari, A; Pichot, C. *Colloid Polym. Sci.* **1999**, *277*, 846−855.
(33) Sauzedde, F.; Elaissari, A; Pichot, C *Colloid Polym. Sci.* **1999**, *277*, 1041−1050.
(34) Rahman, M. M.; Chehimi, M. M.; Fessi, H.; Elaissari, A. *J. Colloid Interface Sci.* **2011**, *360*, 556−564.
(35) Meng, M.; Do Kyung, L.; El Haj, K.; Dobson, A. *J. NanoBioscience, IEEE Trans.* **2009**, *7*, 298−305.
(36) Sulek, S.; Mammadov, B.; Mahcicek, D. I.; Sozeri, H.; Atalar, E.; Tekinay, A. B.; Guler, M. O. *J. Mater. Chem.* **2011**, *21*, 15157−15162.
(37) Martina, M. S.; Fortin, J. P.; Menager, C.; Clement, O.; Barratt, G.; Grabielle-Madelmont, C.; Gazeau, F.; Cabuil, V.; Lesieur, S. *J. Am. Chem. Soc.* **2005**, *127*, 10676−10685.
(38) Yang, X.; Pilla, S.; Grailer, J. J.; Steeber, D. A.; Gong, S.; Chen, Y.; Chen, G. *J. Mater. Chem.* **2009**, *19*, 5812−5817.
(39) Park, J.; Yu, M. K.; Jeong, Y. Y.; Kim, J. W.; Lee, K.; Phan, V. N.; Jon, S. *J. Mater. Chem.* **2009**, *19*, 6412−6417.
(40) Patel, D.; Moon, J. Y.; Chang, Y.; Kim, T. J.; Lee, G. H. *Colloids Surf., A* **2008**, *313−314*, 91−94.
(41) Vekas, L.; Tombacz, E.; Turcu, R.; Morjan, I.; Avdeev, M. V.; Krasia-Christoforou, T.; Socoliuc, V. Synthesis of Magnetic Nanoparticles and Magnetic Fluids for Biomedical Applications. In *Nanoscale Drug Delivery/Drug Design in Nanomedicine − Basic and Clinical Applications in Diagnostics and Therapy* ; Alexiou, C,, Ed.; Else Kröner-Fresenius Symposium; Karger: Basel, Switzerland, 2011; Vol. 2, pp 35−52.
(42) Kötitz, R.; Weitschies, W.; Trahms, L.; Semmler, W. *J. Magn. Magn. Mater.* **1999**, *201*, 102−104.
(43) Papaphilippou, P. C.; Pourgouris, A.; Marinica, O.; Taculescu, A.; Athanasopoulos, G. I.; Vekas, L.; Krasia-Christoforou, T. *J. Magn. Magn. Mater.* **2011**, *323*, 557−563.
(44) Lutz, J. F. *J. Polym. Sci., Part A: Polym. Chem.* **2008**, *46*, 3459−3470.

(45) Papaphilippou, P.; Loizou, L.; Popa, N. C.; Han, A.; Vekas, L.; Odysseos, A.; Krasia-Christoforou, T. *Biomacromolecules* **2009**, *10*, 2662−2671.
(46) Pich, A.; Bhattacharya, S.; Lu, Y.; Boyko, V.; Adler, H. J. P. *Langmuir* **2004**, *20*, 10706−10711.
(47) Bhattacharya, S.; Eckert, F.; Boyko, V.; Pich, A. *Small* **2007**, *3*, 650−657.
(48) Bruining, M. J.; Blaauwgeers, H. G. T.; Kuijer, R.; Pels, E.; Nuijts, R. M. M. A.; Koole, L. H. *Biomaterials* **2000**, *21*, 595−604.
(49) Adams, D. J.; Butler, M. F.; Weaver, A. C. *Langmuir* **2006**, *22*, 4534−4540.
(50) Bica, D. *Rom. Rep. Phys.* **1995**, *47*, 265−270.
(51) Vekas, L.; Bica, D.; Avdeev, M. V. *China Particuol.* **2007**, *5*, 43−49.
(52) Vekas, L.; Avdeev, M. V.; Bica, D. Magnetic Nanofluids: Synthesis and Structure. In *NanoScience in Biomedicine*; Shi, D., Ed.; Springer, New York, 2009; Chapter 25, pp 645.
(53) Feoktystov, V.; Avdeev, M. V.; Aksenov, V. L.; Bulavin, L. A.; Bica, D.; Vekas, L.; Garamus, V. M. *J. Colloid Interface Sci.* **2009**, *334*, 37−41.
(54) Krasia, T.; Patrickios, C. S. *Macromolecules* **2006**, *39*, 2467−2473.
(55) Tombacz, E.; Majzik, A.; Horvat, Zs.; Illes, E. *Rom. Rep. Phys.* **2006**, *58*, 281−286.
(56) Cervantes-Uc, J. M.; Cauich-Rodríguez, J. V.; Herrera-Kao, W. A.; Vázquez-Torres, H.; Marcos-Fernández, A. *Polym. Degrad. Stab.* **2008**, *93*, 1891−1900.
(57) Starodubtsev, S. G.; Saenko, E. V.; Dokukin, M. E.; Aksenov, V. L.; Klechkovskaya, V. V.; Zanaveskina, I. S.; Khokhlov, A. R. *J. Phys.: Condens. Matter* **2005**, *17*, 1471−1480.
(58) Gong, T.; Yang, D.; Hu, J.; Yang, W.; Wang, C.; Lu, J. Q. *Colloids Surf., A* **2009**, *339*, 232−239.
(59) Wan, S.; Zheng, Y.; Liu, Y.; Yan, H.; Liu, K. *J. Mater. Chem.* **2005**, *15*, 3424−3430.
(60) Loizou, E.; Triftaridou, A. I.; Georgiou, T. K.; Vamvakaki, M.; Patrickios, C. S. *Biomacromolecules* **2003**, *4*, 1150−1160.
(61) Sutani, K.; Kaetsu, I.; Uchida, K.; Matsubara, Y. *Radiat. Phys. Chem.* **2002**, *64*, 331−336.